Meltem Tetik
Fırat Parlak
Akım Metal A.Ş. R&D Center, İstanbul-Turkey
ttkmeltem@gmail.com; fparlak@akimmetal.com.tr

DOI	http://dx.doi.org/10.12739/NWSA.2017.12.4.2A0128	
ORCID ID	0000-0002-2614-9618	0000-0001-6072-4578

VELOCITY VECTOR CONTROLLED S-CURVE MOTION PROFILE IN PERMANENT MAGNET SYNCHRONOUS MACHINE (PMSM)

ABSTRACT
In this paper, velocity vector control of the space vector pulse width modulation technique of the field oriented controlled(FOC) permanent magnet brushless synchronous motor(PMSM) will be provided according to asymmetric S-curve motion profile. The equations of S-curve motion profiles and their models are obtained in MATLAB/Simulink. The flow-chart of the algorithms and their implementations are proposed and they are compared. In order to realize high precision control at high speed, the acceleration and deceleration control are discussed in detail and adopted. The experimental results are presented based on TMS320x28xxx. The control becomes more flexible. Simulation and experimental results show that the proposed approach of asymmetric S-curve profile method is more useful for fast, less jerk, vibration-less and smooth motion. So that the best dynamical performance of the motor is achieved.
Keywords: Permanent Magnet Synchronous Machine, Vector Control, Speed Control, S-Curve, TMS320x28xxx

1. INTRODUCTION
Synchronous motors are used extensively in the industry due to their high torque-power values, quiet operation and high efficiency. Various control methods have been developed in permanent magnet motors, which are becoming increasingly common in parallel with improvements in semiconductor technology. Besides the traditional control methods, the vector control and direct torque control methods has also begun to be used in these types of motors. The stator of the synchronous motors has a three-phase winding like the induction motor. By using a permanent magnet instead of a winding on the rotor, the problems caused by the brush and the collector are also eliminated [1]. The use of high-energy permanent magnets in the rotor ensures that the efficiency is higher than the same power synchronous motor by removing the copper losses from the rotor windings. Despite these advantages of permanent magnet synchronous motors, they need an additional drive system using position sensor in torque and speed control [2].
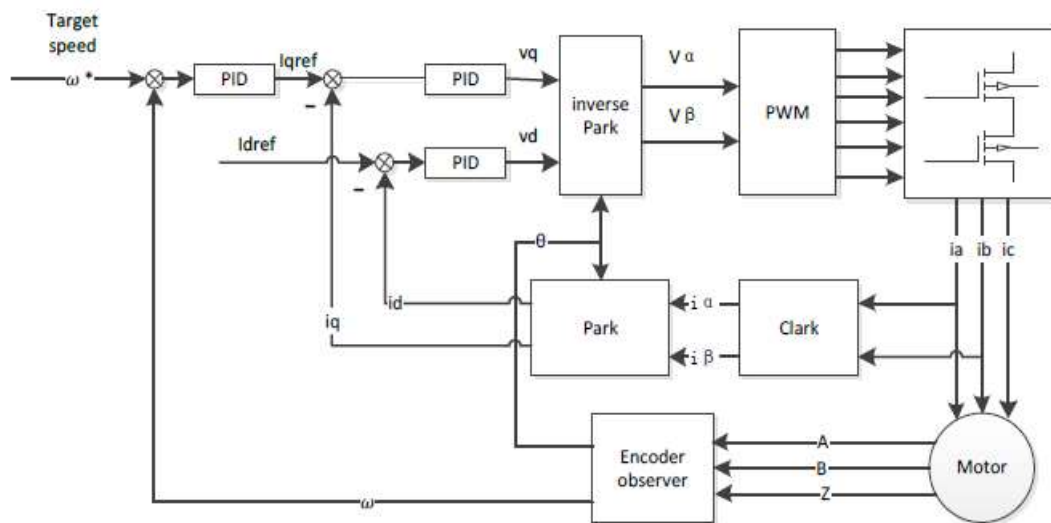
Figure 1. Speed control of permanent magnet brushless synchronous motor [3]

2. RESEARCH SIGNIFICANCE

In this study, speed control of the permanent magnet synchronous motor (PMSM) is achieved by using space vector pulse width modulation (SVPWM) technique, one of the advanced pulse width modulation (PWM) techniques. Many studies have been done on this technique and articles have been published. Due to the high performance characteristics of SVPWM, its usage area has been increasing in recent years. The equations of motion profiles for speed control are obtained and used both in simulation environment and experimental work. The control algorithm of the motor control is implemented by using TMS320x28xxx series of Texas Instruments' microcontroller. The obtained control algorithms for this paper will not only be used for PMSM motors, but also for industrial electric motor drive systems and controls.

In this study, a mathematical model of the permanent magnet brushless synchronous motor with respect to the stator and rotor reference frames is obtained. The equations of space vector pulse width modulation technique for motor control are obtained and the control algorithms are proposed in MATLAB/Simulink. The real-time implementation of the control algorithms is performed by using TMS320x28xxx microcontroller.

3. PERMANENT MAGNET BRUSHLESS SYNCHRONOUS MACHINE MATHEMATICAL MODEL

The mathematical model of the permanent magnet brushless synchronous motor is stated in two frames, the stator reference frame and the rotor reference frame.

3.1. Modeling of Permanent Magnet Brushless Synchronous Motor in Stator Reference Frame

The motor is assumed to be sinusoidal wave current supplied and star connected when the mathematical model of the stator reference frame is derived. The three-phase stator equivalent circuit for the star-connected motor is as given in Figure 2.
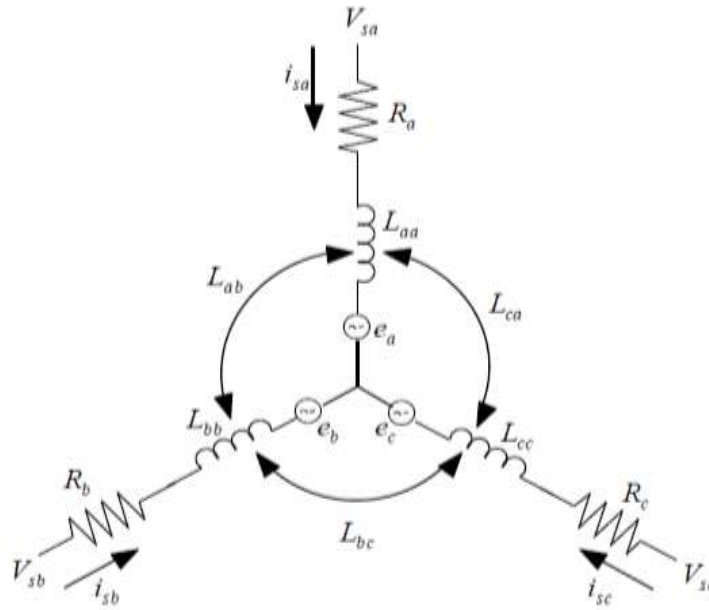
Figure 2. Three-phase equivalent circuit of a permanent magnet synchronous motor [3]

V_{sa}, V_{sb} and V_{sc} voltages are applied to the phase windings of the motor and the i_{sa}, i_{sb} and i_{sc} currents flow through the phase windings. R_a, R_b, R_c represent stator phase winding resistances, L_{aa}, L_{bb}, L_{cc} stator phase winding inductances, L_{ab}, L_{bc}, L_{ca} inductances between stator phases and e_a, e_b, e_c represent back emf which occurs in the stator windings. Stator voltages can be written as in Equation-1 from Figure 2.

$$\begin{bmatrix} V_{sa} \\ V_{sb} \\ V_{sc} \end{bmatrix} = \begin{bmatrix} R_a & 0 & 0 \\ 0 & R_b & 0 \\ 0 & 0 & R_c \end{bmatrix} \begin{bmatrix} i_{sa} \\ i_{sb} \\ i_{sc} \end{bmatrix} + \frac{d}{d_t} \begin{bmatrix} L_{aa} L_{ab} L_{ac} \\ L_{ba} L_{bb} L_{bc} \\ L_{ca} L_{cb} L_{cc} \end{bmatrix} \begin{bmatrix} i_{sa} \\ i_{sb} \\ i_{sc} \end{bmatrix} + \begin{bmatrix} e_a \\ e_b \\ e_c \end{bmatrix} \quad (1)$$

The back emf is dependent on the magnetic flux of the rotor magnet and the rotor speed, and can be expressed by Equation-2.

$$\begin{bmatrix} e_a \\ e_b \\ e_c \end{bmatrix} = -\omega_r \begin{bmatrix} \psi_m (\sin\theta_r) \\ \psi_m (\sin(\theta_r - {}^{2\pi}/_3)) \\ \psi_m (\sin(\theta_r - {}^{4\pi}/_3)) \end{bmatrix} \quad (2)$$

Hence the motor is star connected and the windings are equal and balanced with each other, it can be written as $R_a = R_b = R_c = R$, $L_a = L_b = L_c = L$, $L_{ab} = L_{ac} = L_{bc} = L_{ba} = L_{ca} = L_{cb} = M$.

$$\begin{bmatrix} V_{sa} \\ V_{sb} \\ V_{sc} \end{bmatrix} = \begin{bmatrix} R & 0 & 0 \\ 0 & R & 0 \\ 0 & 0 & R \end{bmatrix} \begin{bmatrix} i_{sa} \\ i_{sb} \\ i_{sc} \end{bmatrix} + \frac{d}{d_t} \begin{bmatrix} L-M & 0 & 0 \\ 0 & L-M & 0 \\ 0 & 0 & L-M \end{bmatrix} \begin{bmatrix} i_{sa} \\ i_{sb} \\ i_{sc} \end{bmatrix} - \omega_r \begin{bmatrix} \psi_m (\sin\theta_r) \\ \psi_m (\sin(\theta_r - {}^{2\pi}/_3)) \\ \psi_m (\sin(\theta_r - {}^{4\pi}/_3)) \end{bmatrix} \quad (3)$$

3.2.   Modeling of Permanent Magnet Brushless Synchronous Motor in Rotor Reference Frame

Clarke and Park transformations are used to construct the mathematical model of the three-phase motor according to the rotor reference frame. The model obtained by the transformations resembles the separately excited DC motor.
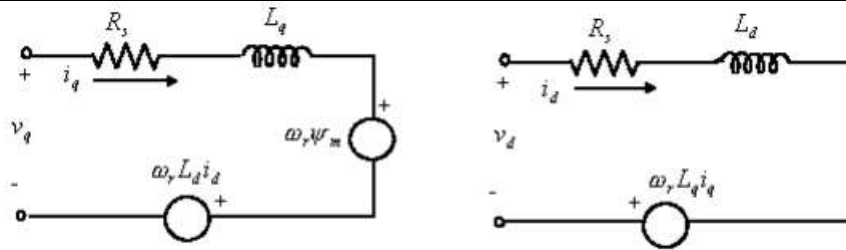
Figure 3. D-Q axis equivalent circuit of the permanent magnet
synchronous motor [3]

The d-q axis voltage equations of the motor according to Figure-3 are given in Equation [4 and 5].

$$V_d = Ri_d + L_d \frac{di_d}{dt} - \omega_r L_q i_q \qquad (4)$$

$$V_q = Ri_q + L_q \frac{di_q}{dt} + \omega_r L_d i_d + \omega_r \psi_m \qquad (5)$$

The d-q axis magnetic flux equations are given in Equation [6 and 8].

$$\psi_d = L_d i_d + \psi_m \qquad (6)$$

$$\psi_q = L_q i_q \qquad (7)$$

$$\begin{bmatrix} V_d \\ V_q \end{bmatrix} = \begin{bmatrix} R & 0 \\ 0 & R \end{bmatrix} \begin{bmatrix} i_d \\ i_q \end{bmatrix} + \frac{d}{dt} \begin{bmatrix} L_d & 0 \\ 0 & L_q \end{bmatrix} \begin{bmatrix} i_d \\ i_q \end{bmatrix} + \omega_r \begin{bmatrix} -L_q i_q \\ L_d i_d + \psi_m \end{bmatrix} \qquad (8)$$

V_d is expressed as d-axis voltage, V_q q-axis voltage, i_d d-axis current, i_q q-axis current, ω_r rotor speed, ψ_m magnetization current, ψ_d d-axis magnetic flux, ψ_q q-axis magnetic flux.

4. SPACE VECTOR PULSE WIDTH MODULATION

In the performance of permanent magnet brushless synchronous motor drivers, the modulation technique used for switching is of great importance. SVPWM technique has advantages as very good harmonic performance, broadening of the modulation index range, optimum use of direct current input voltage and low current ripple [4 and 5]. The appropriate choice of small space vectors and the equal switching time and starting and ending states of the switching sequences provide advantages such as low voltage ripple and low total harmonic distortion. The SVPWM technique uses a similar sequence. Therefore their performance is better than other pulse width modulation techniques. Thus, the space vector pulse width modulation technique has a higher linear modulation rate than other pulse width modulation techniques [6].
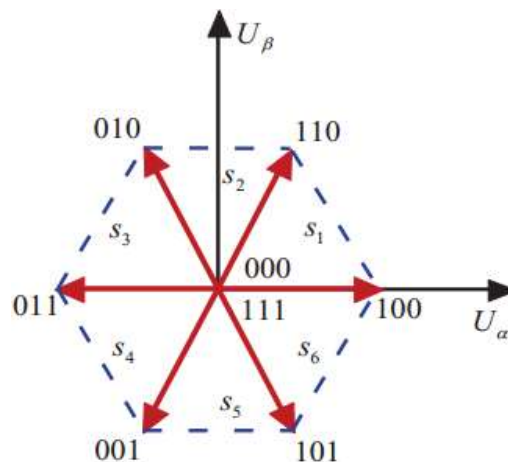

Figure 4. Space vector pulse width modulation vector diagram [7]

In the SVPWM technique, the three-phase reference currents are represented by the current space vector in the α-β space using the Clarke transformation. The length of the vector and the phase angle are calculated by the instantaneous values of these three-phase components. If the three-phase components are sinusoidal and balanced, the vector will rotate at a constant angular velocity and will have a fixed length. In other words, a rotating voltage vector will form. The SVPWM technique is constructed by taking all the reference vectors (Vref) in the hexagon, the weighted averages of the two space vectors adjacent to Vref and the zero vectors [8]. In Figure 5, the Vref voltage vector and the components of this vector are shown, for example, in the first sector.
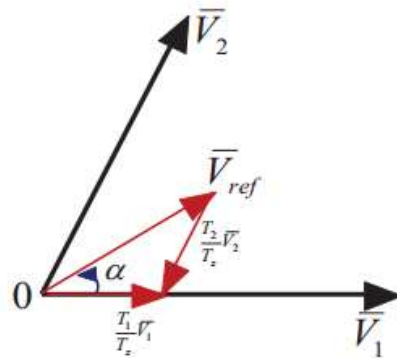

Figure 5. Reference voltage vector in sector-1 [7]

The V_ref voltage vector on α-β frame is expressed as in Equation 9.

$$V_{ref} = V_\alpha + V_\beta = \frac{2}{3}\left(V_a + V_b e^{j2\pi/3} + V_c e^{j4\pi/3}\right) \tag{9}$$

The values of the six voltage vectors, which each sector will have in the border region, are as given in Equation 10.

$$V_k = \frac{2}{3}V_{dc}e^{-j(k-1)\pi/3} \qquad k = 1, \dots, 6 \tag{10}$$

k is the sector number.

Ts is chosen as switching period for the space vector PWM technique. Equation [11 and 15] gives the equations related to the calculation of the reference voltage over a period.

$$\int_0^{T_s/2} V_{ref}\,dt = \int_0^{T_0/2} V_0\,dt + \int_{T_0/2}^{T_k+T_0/2} V_k\,dt + \int_{T_k+T_0/2}^{T_k+T_{k+1}+T_0/2} V_{k+1}\,dt + \int_{T_k+T_{k+1}+T_0/2}^{T_s/2} V_7\,dt \tag{11}$$

$$T_0 + T_k + T_{k+1} = \frac{T_s}{2} \tag{12}$$

$$V_0 + V_7 = 0 \tag{13}$$

$$V_{ref}\frac{T_s}{2} = V_k T_k + V_{k+1} T_{k+1} \tag{14}$$

$$V_{ref} = \frac{2}{3}V_{dc}e^{-j(k-1)\frac{\pi}{3}}\frac{T_k}{T_s/2} + \frac{2}{3}V_{dc}e^{-jk\frac{\pi}{3}}\frac{T_{k+1}}{T_s/2} \tag{15}$$

The voltage vectors for the α-β frame are expressed as in Equation-16. Where T_k ve T_{k+1} represent the operating duration of the components of the reference voltage vector and are calculated as shown in Equation 17.

$$\begin{bmatrix} V_\alpha \\ V_\beta \end{bmatrix}\frac{T_s}{2} = \frac{2}{3}V_{dc}\begin{bmatrix} \cos(k-1)\pi/3 & \cos k\pi/3 \\ \sin(k-1)\pi/3 & \sin k\pi/3 \end{bmatrix}\begin{bmatrix} T_k \\ T_{k+1} \end{bmatrix} \tag{16}$$

$$\begin{bmatrix} T_k \\ T_{k+1} \end{bmatrix} = \frac{\sqrt{3}}{2}\frac{T_s}{V_{dc}}\begin{bmatrix} \cos(k-1)\pi/3 & \cos k\pi/3 \\ \sin(k-1)\pi/3 & \sin k\pi/3 \end{bmatrix} \tag{17}$$

In space vector PWM technique, the active and cutoff times of the used semiconductors are obtained by some calculations. Active and cut-off conditions of the switches and α, β voltages are given in Table 1.

Table 1. α, β voltages according to switching states [9]

	S1	S3	S5	U_α	U_β	U_{ref}	Vector
000	OFF	OFF	OFF	0	0	0	V_0
001	OFF	OFF	ON	$-U_{DC}/3$	$-U_{DC}\sqrt{3}$	$2U_{DC}/3$	V_1
010	OFF	ON	OFF	$-U_{DC}/3$	$U_{DC}\sqrt{3}$	$2U_{DC}/3$	V_2
011	OFF	ON	ON	$-2U_{DC}/3$	0	$2U_{DC}/3$	V_3
100	ON	OFF	OFF	$2U_{DC}/3$	0	$2U_{DC}/3$	V_4
101	ON	OFF	ON	$U_{DC}/3$	$-U_{DC}\sqrt{3}$	$2U_{DC}/3$	V_5
110	ON	ON	OFF	$U_{DC}/3$	$U_{DC}\sqrt{3}$	$2U_{DC}/3$	V_6
111	ON	ON	ON	0	0	0	V_7

The switching states for the three-phase, two-level SVPWM inverter are shown in Figure 6. There are a total of eight switching states depending on the active and cut-off states of the parent keys. The inverter output voltage is also due to the combination of these eight switching states.
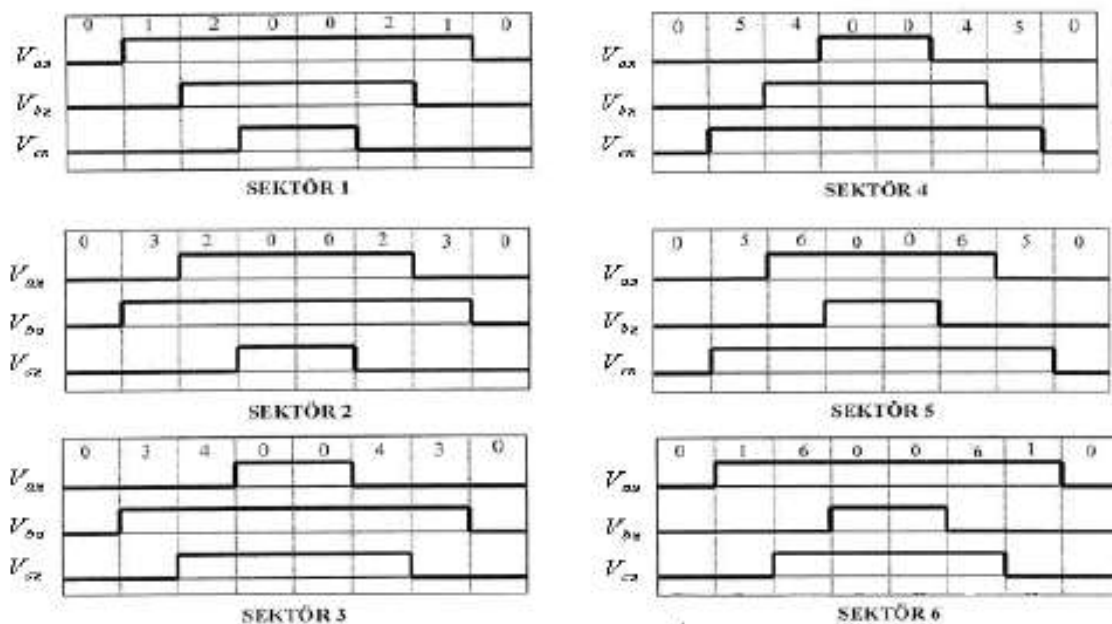

Figure 6. PWM states of the phases for the six sectors [10]

5. S-CURVE MOTION PROFILES
Two different speed profiles will be used when speed control of the permanent magnet brushless synchronous motor is performed.

5.1. S-Curve Speed Reference
The S-curve speed reference to be used for the speed control of the permanent magnet brushless synchronous motor is as in Figure 7.
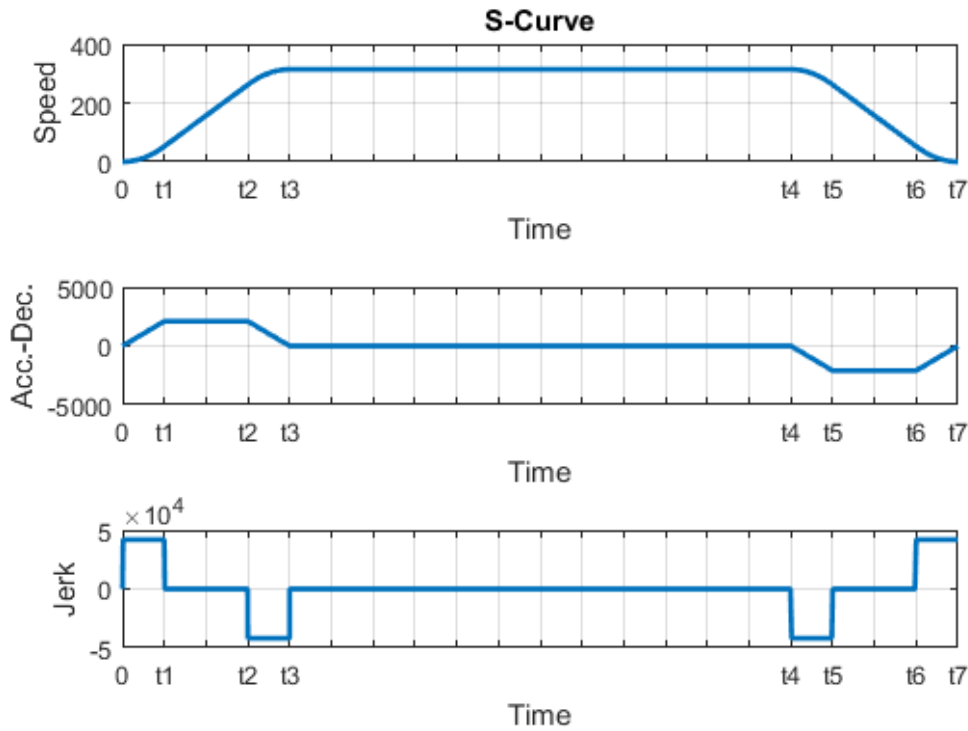
Figure 7. S-curve speed profile

Jerk(J) is calculated and s-curve speed profile is created. Equation [18 and 19] is used for the S-curve speed profile [11].

$$J(t) = \begin{cases} J & 0 \le t < t_1 \\ 0 & t_1 \le t < t_2 \\ -J & t_2 \le t < t_3 \\ 0 & t_3 \le t < t_4 \\ -J & t_4 \le t < t_5 \\ 0 & t_5 \le t < t_6 \\ J & t_6 \le t < t_7 \end{cases} \tag{18}$$

$$V(t) = \begin{cases} V_s + 0.5J(t_1 - 0)^2 & 0 \le t < t_1 \quad t = t_1 & V_{01} = V_s + 0.5JT_1^2 \\ V_{01} + JT_1(t_2 - t_1) & t_1 \le t < t_2 \quad t = t_2 & V_{02} = V_{01} + JT_1T_2 \\ V_{02} + JT_1(t_3 - t_2) - 0.5J(t_3 - t_2)^2 & t_2 \le t < t_3 \quad t = t_3 & V_{03} = V_{02} + 0.5JT_1^2 \\ V_{03} & t_3 \le t < t_4 \ , \ t = t_4 & V_{04} = V_{03} \\ V_{04} - 0.5J(t_5 - t_4)^2 & t_4 \le t < t_5 \quad t = t_5 & V_{05} = V_{04} - 0.5JT_5^2 \\ V_{05} - JT_5(t_6 - t_5) & t_5 \le t < t_6 \quad t = t_6 & V_{06} = V_{05} - JT_5T_6 \\ V_{06} - JT_5(t_7 - t_6) + 0.5J(t_7 - t_6)^2 & t_6 \le t < t_7 \quad t = t_7 & V_{07} = V_{06} - 0.5JT_5^2 \end{cases} \tag{19}$$

5.2. Asymmetric S-Curve Speed Reference

The asymmetric S-curve speed reference to be used for speed control of the permanent magnet brushless synchronous motor is as in Figure 8.
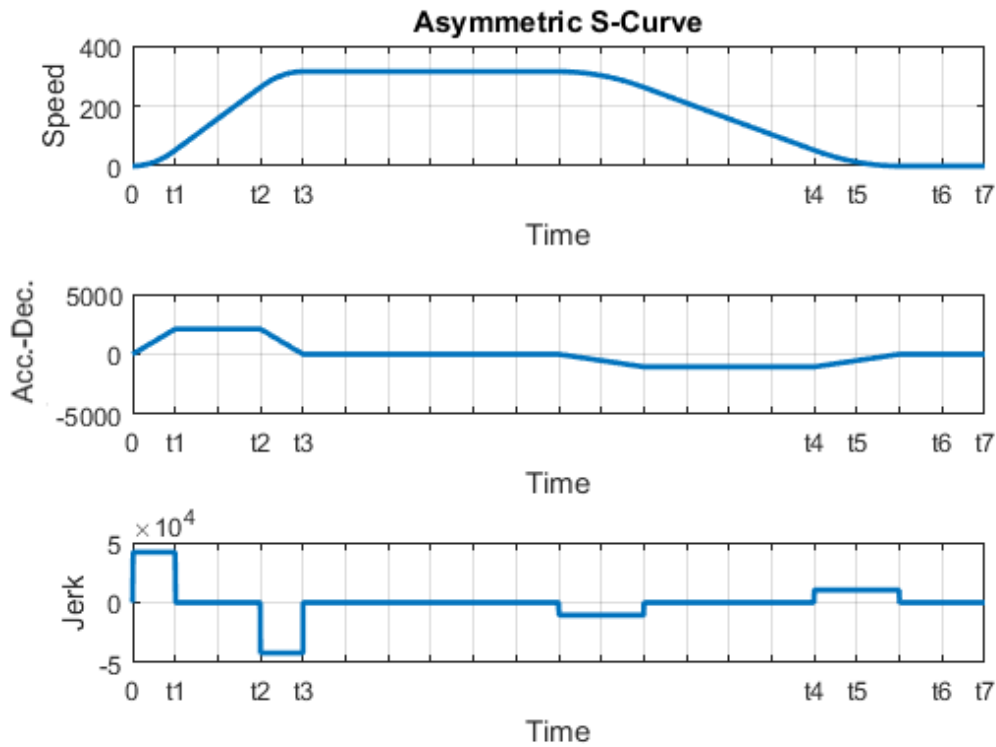
Figure 8. Asymmetric S-Curve speed profile

The asymmetric s-curve speed profile is calculated by calculating Jerk (J). Equation [20 and 21] is used for the asymmetric s-curve speed profile [12].

$$
J(t) = \begin{cases}
J_1 & 0 \le t < t_1 \\
0 & t_1 \le t < t_2 \\
-J_1 & t_2 \le t < t_3 \\
0 & t_3 \le t < t_4 \\
-J_2 & t_4 \le t < t_5 \\
0 & t_5 \le t < t_6 \\
J_2 & t_6 \le t < t_7
\end{cases}
\tag{20}
$$

$$
V(t) = \begin{cases}
V_s + 0.5J_1(t_1 - 0)^2 & 0 \le t < t_1 & t = t_1 & V_{01} = V_s + 0.5JT_1^2 \\
V_{01} + J_1T_1(t_2 - t_1) & t_1 \le t < t_2 & t = t_2 & V_{02} = V_{01} + JT_1T_2 \\
V_{02} + J_1T_1(t_3 - t_2) - 0.5J_1(t_3 - t_2)^2 & t_2 \le t < t_3 & t = t_3 & V_{03} = V_{02} + 0.5JT_1^2 \\
V_{03} & t_3 \le t < t_4 , & t = t_4 & V_{04} = V_{03} \\
V_{04} - 0.5J_2(t_5 - t_4)^2 & t_4 \le t < t_5 & t = t_5 & V_{05} = V_{04} - 0.5JT_5^2 \\
V_{05} - J_2T_5(t_6 - t_5) & t_5 \le t < t_6 & t = t_6 & V_{06} = V_{05} - JT_5T_6 \\
V_{06} - J_2T_5(t_7 - t_6) + 0.5J_2(t_7 - t_6)^2 & t_6 \le t < t_7 & t = t_7 & V_{07} = V_{06} - 0.5JT_5^2
\end{cases}
\tag{21}
$$

In equations 18 and 21, $T_1 = (t_1 - t_0)$, $T_5 = (t_5 - t_4)$ are abbreviated.

6. SIMULATION AND EXPERIMENTAL METHOD-PROCESS

In this section, a simulation and experimental study on the speed control of the permanent magnet synchronous motor in the MATLAB/Simulink program using the space pulse width modulation technique is described. The general structure of the motor control algorithm is given in Figure 9.
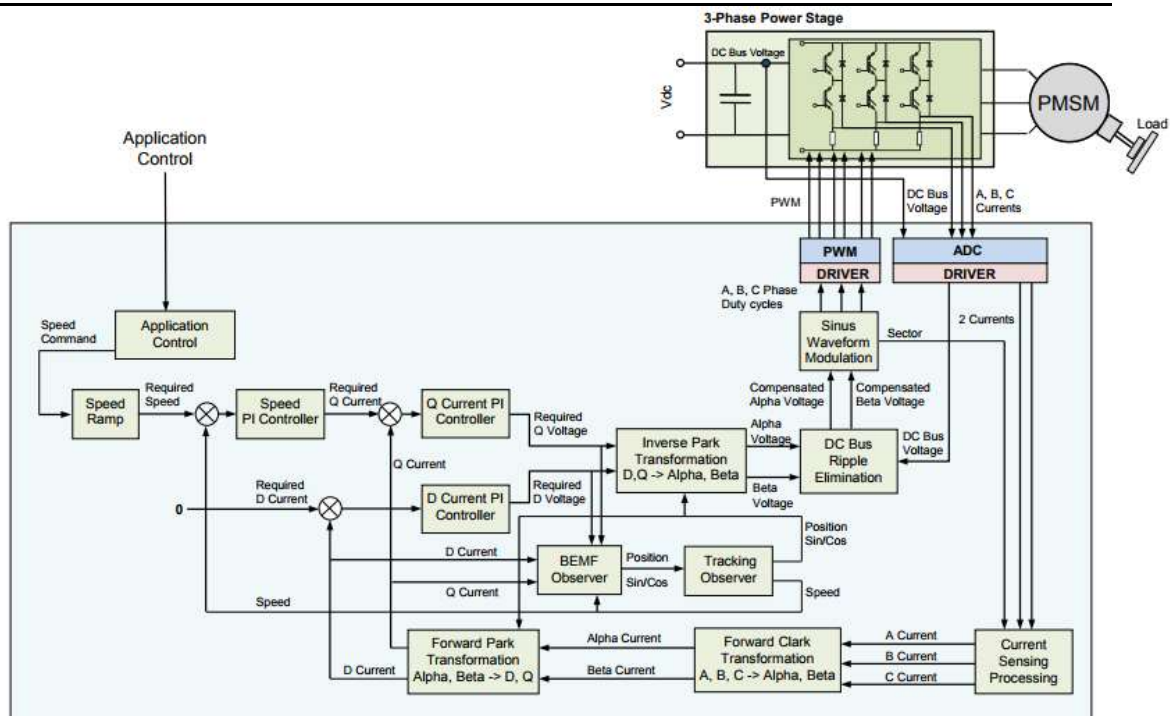
Figure 9. Permanent magnet brushless synchronous motor control algorithm

SM080-075 motor is used in the simulation of the control algorithm and in the experimental work. The motor parameters are as given in Table 2. System behaviors are observed by applying S-curve motion profiles as speed reference.

Table 2. Parameters of permanent magnet brushless synchronous motor [13 and 14]

Rated Speed	w (rpm)	3000
Rated Torque	T (Nm)	2.4
Rated Current	I (Arms)	5
Stator Resistance (Phase-Phase)	R (Ω)	0.713
Inductance (Phase-Phase)	L (H)	0.00613
Pole Pair	P	5
Magnet Flux	ψ (V.s)	0.045255
Inertia	J ($kg \, x \, m^2$)	0.00011
Viscous Damping	F (Nms)	$4.047 x 10^{-5}$

6.1. Simulation Results
The speed control with space vector pulse width modulation (SVPWM) of permanent magnet brushless synchronous motor is simulated in MATLAB/Simulink program. Figure 10 shows the MATLAB/Simulink model for system control.
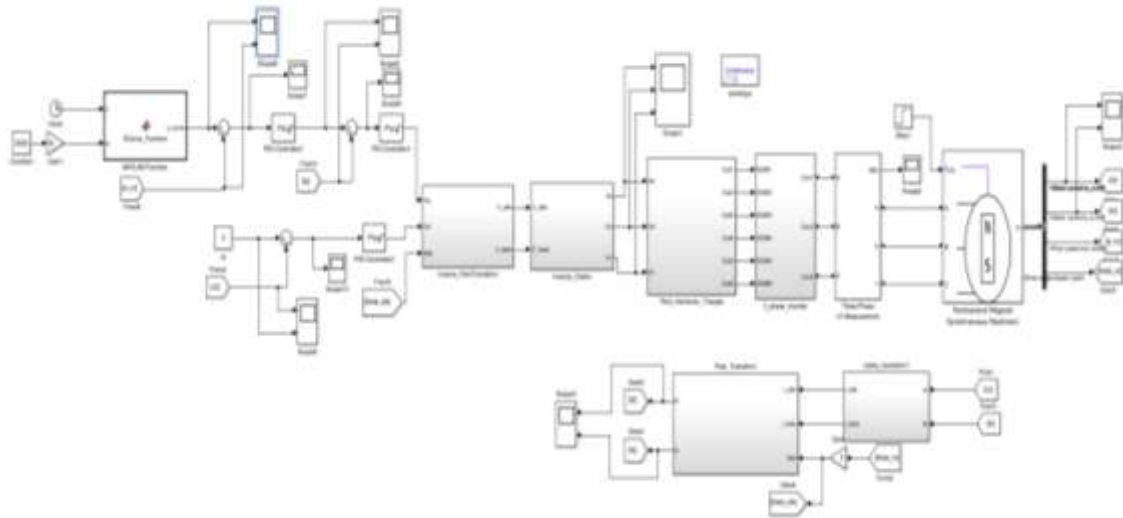
Figure 10. Speed control of the permanent magnet synchronous motor

When the S-curve speed reference is used as the reference speed profile in the system, it is observed that there is no overshoot when the speed reaches the rated speed. When the motor is at rated speed and loaded with rated torque, a 4.66rad/s collapse is observed at speed and the speed has reached the reference at 40ms. When the S-curve motion profile is applied, the q-axis current in the acceleration and deceleration region is observed to oscillate 2.5 Arms.
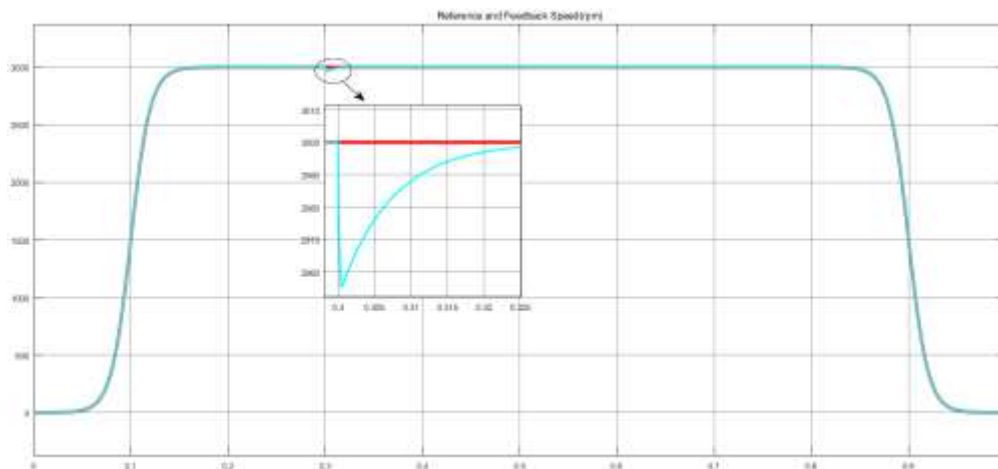

Figure 11. S-Curve speed reference and feedback (rpm)

When the asymmetric S-curve speed reference is used as the reference speed profile in the system, it is observed that there is no overshoot when the speed reaches the rated speed. When the motor is at rated speed and loaded with rated torque, 4.66rad/s collapse is observed at speed and it is seen that the reference of speed is reached at 30ms. When the S-curve motion profile is applied, it is observed that the q-axis current is oscillated at 2.5 Arms in the acceleration region and at 0.5 Arms in the deceleration region.
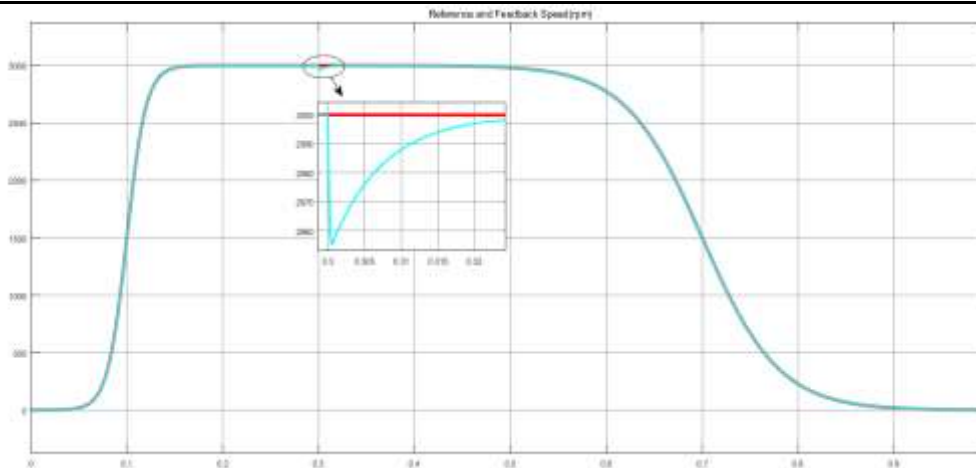
Figure 12. Asymmetric S-Curve speed reference and feedback (rpm)

6.2. Experimental Results

To provide speed control with space vector pulse width modulation (SVPWM) of permanent magnet brushless synchronous motor, the TMS320x28xxx series microcontroller is used in the control card which is designed at R&D Center. The microcontroller has a maximum operating frequency of 90MHz and has a variety of peripherals (ADC, eQEP, ePWM, eCAP, etc.) customized for motor applications. The experimental setup used for this study is given in Figure 13. The control card designed with TMS320x28xxx series microcontroller is given in Figure 14.
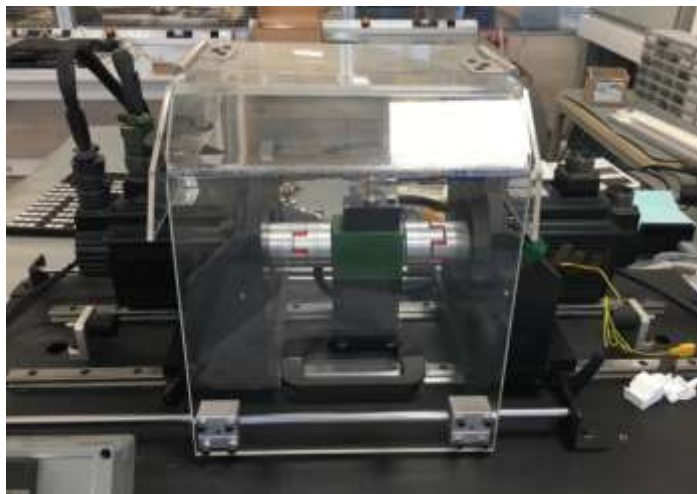

Figure 13. The experimental setup

Figure 14. Control card with TMS320x28xxx microcontroller

In order to load the test equipment, ECMA motor and ASDA-A2 series driver of Delta Company are used. Speed control of the SM080-075 motor is carried out with the designed control card using the TMS320x28xxx series microcontroller. Experimental study of the control algorithm is performed by writing codes in C language using the space pulse width modulation technique equations in Section 4 and the motion profile equations in Section 5. Two different S-curve motion profiles have been created to provide motor speed control. For S-curve speed profile; the time from zero speed to rated speed (3000rpm) is set to 200ms, the duration of the rated speed to 600ms and from the rated speed to zero speed to 200ms. For asymmetric S-curve speed profile; the time from zero speed to the rated speed (3000rpm) is set to 200ms, the duration of the rated speed to 300ms and from the rated speed to zero speed to 400ms. The reference signal generated for motor control and the speed information of the motors is plotted using Excel. Figure-15 shows the speed signal obtained when the S-curve motion profile is applied. Figure 16 shows the speed signal obtained when the asymmetric S-curve motion profile is applied. On both profiles, when loaded with rated torque at rated speed, a 5 rad/s collapse is observed at speed.
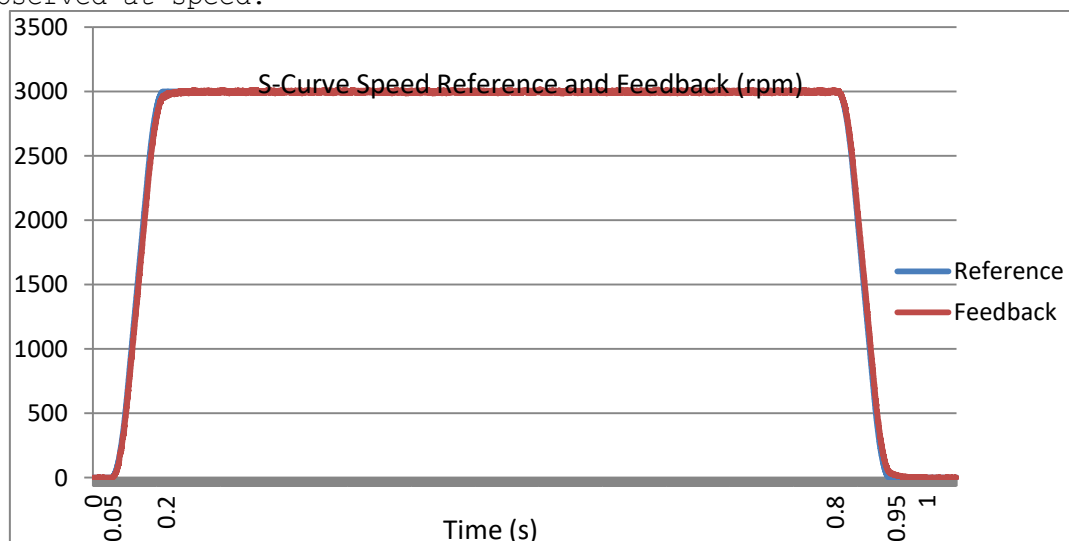

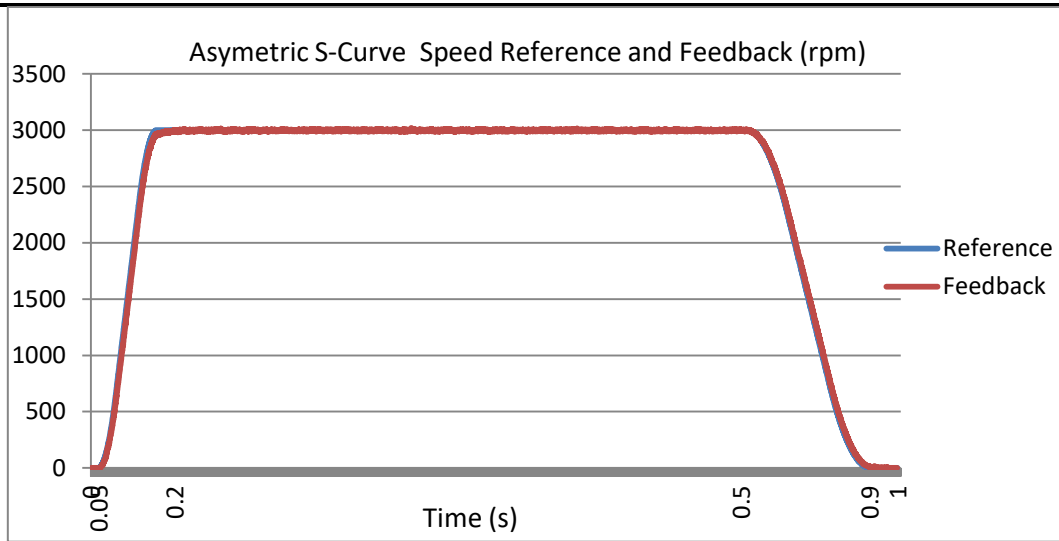
Figure 15. S-Curve speed reference and feedback (rpm)

Figure 16. Asymmetric S-Curve speed reference and feedback (rpm)

For the reference speed profiles used in the experimental study, the acceleration graph is given in Figure 17 and the jerk graph is given in Figure 18. In the experimental study, when the asymmetric s-curve motion profile is applied, the effect of the Jerk formed in the system is shown in Figure 18, and it is observed that the ripple is less in the current.
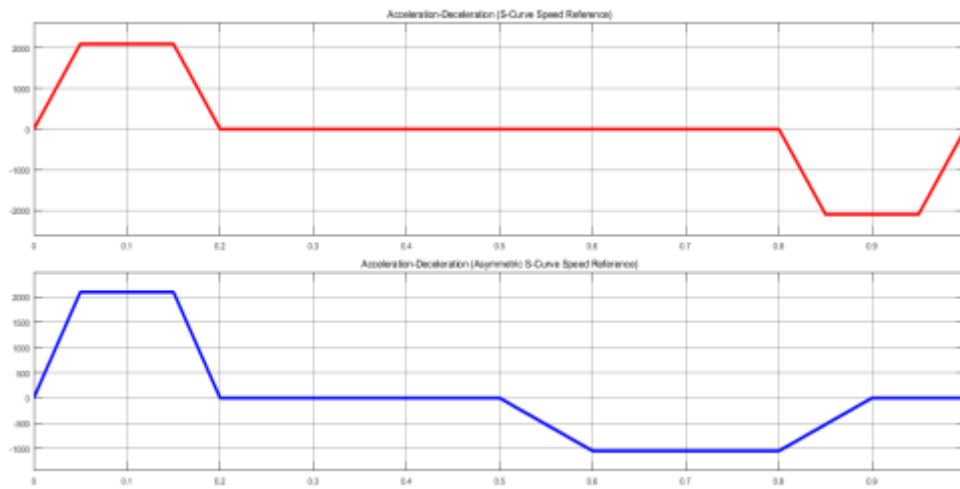

Figure 17. Acceleration-Deceleration graph according to reference speed profiles
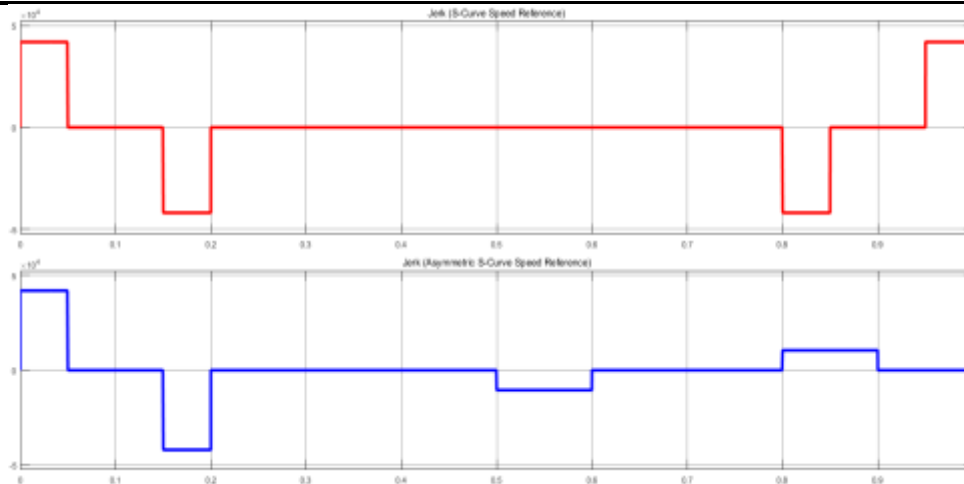
Figure 18. Jerk graph according to reference speed profiles

7. CONCLUSION AND RECOMMENDATIONS

The speed control with space vector pulse width modulation of the permanent magnet brushless synchronous motor has been performed for two different S-curve velocity profiles. Simulation and experimental study are carried out using the same controller coefficients in two different speed profiles. As a result of simulation and experimental study, it is observed that there is no overshoot in speed profile when both speed profiles reach the reference speed. S-curve or asymmetric S-curve speed references can be used to prevent vibrations (oscillations) that may occur due to jerk in the system. Asymmetric S-curve speed reference may be preferred in order to reduce the vibration (oscillation) in the deceleration region in the speed control. It has been observed that there is less oscillation in the deceleration region of the asymmetric S-curve. The asymmetric S-curve can be preferred because this allows the generated electrical torque to be more linear.

NOTE

After this study presented as oral presentation at International Science Symposium (ISS2017) in Georgia-Tbilisi between dates 05-08 September 2017, it expanded and restructure.

REFERENCES
1. Pillay, P. and Krishnan, R., (1989). Modelling, Simulation and Analysis of Permanat Magnet Motor Drives, Part 1: The Permanent Magnet Synshronous Motor Drive. IEEE Transactions on Industry Applications, 25(2):265/273.
2. Nasar, S.A., Boldea, I., and Unnewhr, L.E., (1993). Permanent Magnet, Reluctance and Self-Synchronous Motors. CRC Press, USA, 107-215.
3. Asker, M.E., (2009). Sürekli Mıknatıslı Senkron Motorlara Vektör ve Doğrudan Moment Kontrol Yöntemlerinin Uygulanması, Yüksek lisans Tezi, Elazığ: Fırat Üniversitesi Fen Bilimleri Enstitüsü.
4. Rashid, M.H., (2001). Power Electronics Handbook. Academic Press, San Diego, California.
5. Zhou, K. and Wang, D., (2003). Relationship between space vector modulation and three carrier-based PWM: A comprehensive, IEEE Transactions on Industrial. Electronics, 49, 186-196.
6. Rodriguez, J., Gonzalez, A., and Weinstein, A., (2000). Regenerative Cell with Reduced Input Current Harmonics for

Multilevel Inverters. Industry Applications Conference, Vol:1, pp:371-378.
7. TI, (1999). Implementation of a Speed Field Oriented Control of 3- phase PMSM Motor using TMS320F240. Texas Instruments, SPRA588
8. Sul, S., (2011). Control of Electric Machine Drive Systems. Wiley-IEEE Press.
9. Yolaçan, E., (2012). Küçük Güçlü Yüzey Mıknatıslı ve Dahili Mıknatıslı Motorlara Vektör Kontrol Yönteminin Deneysel Olarak Uygulanması. Yüksek Lisans Tezi, Kocaeli: Kocaeli Üniversitesi Fen Bilimleri Enstitüsü.
10. Tetik, M., (2015). Sürekli Mıknatıslı Fırçasız Senkron Motorların SVPWM ile Konum ve Hız Denetimi. Lisans Tezi, Kocaeli: Kocaeli Üniversitesi Mekatronik Mühendsiliği.
11. Kuijing, Z. and Li, C., (2008). Adaptive S-Curve Acceleration/Deceleration Control Method. Proceedings of the 7th World Congress on Intelligent Control Automation, June 25-27, Chongqing, China.
12. Chang-Wan, H., Keun-Ho, R., and Kyung-Soo, K., (2008). A Complete Solution to Asymmetric S-Curve Motion Profile: Theory & Experiments. International Conference on Control, Automation and Systems, Oct. 14-17, Seoul, Korea.
13. http://www.smb-technics.com/tr/.
14. http://www.akimmetal.com.tr/tr/uretim/motor-uretim-3.